Influence of the painting medium on the alteration process of smalt in oil paintings studied using combined K and Co K-edge XANES

Clément de Mecquenem, Myriam Eveno, Damaris Zurbach, Kristina Mösl, Marine Cotte, Ina Reiche

Influence of the painting medium on the alteration process of smalt in oil paintings studied using combined K and Co K-edge XANES.

Clément de MECQUENEM (1,2), Myriam EVENO (3,4), Damaris ZURBACH (2), Kristina Mösl (5), Marine COTTE (6,7) and Ina REICHE (2, 4)

(1) Institut photonique d'analyse non-destructive Européen des matériaux anciens (IPANEMA), CNRS, Ministère de la Culture, UVSQ, MNHN, UAR 3461, Saint-Aubin, France
(2) Laboratoire de développement instrumental et de méthodologies innovantes pour les biens culturels (Lab-BC), C2RMF-CNRS-Chimie Paristech, Université PSL, UAR3506, Paris, France
(3) Centre de Recherche et de Restauration des musées de France (C2RMF), Paris, France
(4) Physicochimie des matériaux témoins de l'histoire, IRCP, CNRS, Chimie Paristech, Université PSL, UMR 8247, Paris, France
(5) Alte Nationalgalerie, Staatliche Museen zu Berlin, Berlin, Germany
(6) European Synchrotron Radiation Facility – Grenoble – France
(7) Laboratoire d'Archéologie Moléculaire et Structurale, University of Sorbonne, Pierre and Marie Curie, University Paris 06, CNRS, UMR 8220, Paris - France

Keywords: Oil paintings, smalt, alteration, medium, XANES.

Abstract

This study investigates the alteration processes affecting the smalt pigment in historical artworks through a combination of analytical techniques including X-ray Absorption Near Edge Structure (XANES) spectroscopy at the potassium (K) and cobalt (Co) K-edges, coupled with scanning electron microscopy with energy-dispersive X-ray spectroscopy (SEM-EDX) and micro X-ray fluorescence elemental mapping (µ-XRF). Laboratory mock-up samples prepared with different oil binding media were artificially aged, revealing varying rates of smalt degradation. µ-XANES analyses at the K K-edge provided grain-scale insights into smalt alteration, highlighting the influence of binding media composition on degradation kinetics. Crossed clustering data analysis over K µ-XANES acquired on both model samples and historical cross-sections corroborated findings and identified distinct spectral signatures associated with different stages of smalt degradation. Furthermore, identification of potential transformation products such as potassium alum in historical samples emphasized the dynamic nature of pigment alteration processes.

Introduction

Over time, historical paintings undergo alterations that result in a modification of their appearance. Some of these alterations, such as the discoloration of smalt, are irreversible and cannot be restored. Smalt, a potassium (K)-rich glass tinted blue by the addition of cobalt (Co), was commonly used as a pigment in oil paintings, murals, and polychromies between the 16th and 18th centuries [1–3].

The hue of this blue pigment varied depending on the size of the grains and the Co concentration, which could range from 1-2% of the total weight of a grain when used as a brightener [1] to 15% in those used as pigment in paintings. The concentration of Co found in this pigment in paintings typically ranged between 3 and 7% [4]. Apart from K and Co, smalt grains also contained various other minor elements depending on the Co ores used for coloring, including arsenic (As), iron (Fe), nickel (Ni), or bismuth (Bi) [5].

However, smalt is known for its tendency to undergo altering in oil paintings, transitioning from a blue to a transparent color, which gives a brownish hue to the paint layer due to the color of the medium. An ionic exchange between H^+ ions from the environment surrounding the grains and K^+ ions from the glass grains is responsible for the alteration. The leaching of K^+ ions leads to several phenomena: firstly, leached K^+ ions can react with the binder, forming K soaps that migrate to the paint surface, creating a crust on the painting. Secondly, the leaching induces a charge deficit around Co^{2+} complexes. This deficit forces the Co^{2+} complexes to rearrange in the glass matrix, shifting from a tetrahedral coordination to an octahedral one, which explains the loss of color in the pigment in paintings [4, 6, 7].

While the alteration mechanism of smalt has been extensively studied and understood, the factors influencing the processes are unclear. Our work focuses on understanding several factors that could affect the alteration process. To achieve this, a comprehensive analysis of the alteration state of smalt in paintings from French museum collections that had been studied by our team based at the *Centre de Recherche et de Restauration des Musées de France* (C2RMF). Surprisingly, our findings revealed that the altering mechanism is not solely dependent on time, and the depth of the smalt-containing paint layer in paintings does not appear to influence the altering of the pigment [8].

The fact that the alteration of smalt does not depend on the depth of its paint layer within the stratigraphy of the painting is intriguing. This indicates that the alteration is not due to proximity to the surface, suggesting that factors such as light or the atmospheric conditions surrounding the painting should play only minimal roles in pigment alteration. The composition of the paint layer containing smalt itself thus likely explains the. The role of other pigments has already been debated, notably that of lead white, which is often cited as potentially protecting smalt from alteration [4, 7]. However, lead white has also been found in mixtures where smalt is in an advanced state of alteration [9].

As a result, our attention shifted to investigating the influence of other components within the smalt-containing paint layer, such as other pigments mixed with smalt or the binding medium. In this article, a discussion on the influence of the binding medium is proposed by preparing, aging, and analyzing mock-up samples that recreate paint layers composed of smalt mixed with different types of oil binders, namely linseed oil and walnut oil siccatived with litharge or not. These samples underwent several analyses to gain insights into their composition and alteration over the aging process. In parallel, the same methods were used for the investigation of a series of selected cross-sections of historical oil paintings to verify that the results obtained on the aged mock-ups represent the processes occurring in historical oil paintings containing smalt.

Initially, scanning electron microscopy with energy-dispersive X-ray spectroscopy (SEM-EDX) was employed to track the composition of smalt grains throughout the aging process for each type of mock-up or historical cross-section. This allowed us to observe any changes in the smalt's grain composition as the mock-ups aged or in the historical sample.

Subsequently, the coordination state of the Co^{2+} ions within the smalt grains was determined by combined K and Co K-edge X-ray absorption near edge spectroscopy (XANES). To our knowledge, this is the first reported use of K K-edge XANES spectra for the study of the degradation process of smalt and its degradation products [10]. These spectra provided precise information about the alteration state of the pigment in the mock-ups and in the historical cross-sections. Particularly, K K-edge XANES probes the changes in the immediate surroundings of K^+ ions during the leaching out of smalt grains, offering a means to explore modifications in the silicate matrix during the alteration process. Additionally, K K-edges XANES

investigates the transformations that K^+ ions undergo in the binding medium, enhancing our understanding of the interaction between K^+ ions and the binding medium of the smalt-based paint layer.

Materials and methods

1. Preparation of mock-up sample

For this study, four sets of smalt mock-up samples were prepared to reproduce smalt-containing paint layers. Deffner & Johann, a German supplier of materials, tools, and equipment for conservation and restoration, provided the smalt used to prepare those samples. This smalt differs from the ancient one without chemical impurities such as arsenic. This smalt was ground with different binders: cooked walnut oil, cooked linseed oil, siccative walnut oil, and siccative linseed oil [11, 12]. Cooked walnut and linseed oil were prepared by heating them between 120 and 130 °C for 4 hours. Siccative oils were prepared by mixing 100g of oil with 100g of distilled water and 10g of lead oxide (PbO) and heating it at 90°C for 3 hours. After the preparation of the media, paints were prepared by grinding 1 g of smalt pigment into 0.5 mL of medium. The resulting paints were then spread on glass slides with a 90 µm thickness. For each preparation set, five mock-up samples were prepared to be artificially aged for different durations.

After one week of drying mock-up samples were artificially aged in a thermostatic oven at 70°C in a vapor-saturated environment and without lighting [13]. While these conditions are designed to maximise the acceleration of the alteration processes, it is important to note that they do not directly replicate the natural aging processes seen in historical samples. If all samples were aged under the same conditions, malfunctions of the thermostatic oven prevented maintaining a constant temperature of 70°C and saturated vapor pressure throughout the entire aging process. The recorded thermostatic conditions, when checking the oven, are summarized in the supplementary materials.

For each set of mock-up samples, one sample was not artificially aged, one aged for three days, one for 11 days, and one for 18 days. Table 1 presents the list of the thirty created and aged samples.

Table 1: list of the mock-up samples

Name	CL		CW		SL		SW	
Binder	Cooked linseed oil		Cooked walnut oil		Siccative linseed oil		Siccative walnut oil	
Aging time	Name	Time	Name	Time	Name	Time	Name	Time
	CL0	0 day	CW0	0 day	SL0	0 day	SW0	0 day
	CL1	3 days	CW1	3 days	SL1	3 days	SW1	3 days
	CL2	8 days	CW2	8 days	SL2	8 days	SW2	8 days
	CL3	15 days	CW3	15 days	SL3	15 days	SW3	15 days
	CL4	23 days	CW4	23 days	SL4	23 days	SW4	23 days

Mock-up samples were prepared as thin sections of 30 µm thickness for the experiment, with the paint layer positioned between a polypropylene plate and a tape that does not contain

sulfur or other elements that could interfere with our analysis.
For SEM-EDX analyses, mock-ups were prepared as cross-sections embedded in polyester resin (SODY33), then cutting with a saw and grinding on silicon carbide (SiC) paper. Polishing was conducted using Micromesh® polishing cloth. For mock-ups CL4, CW4, and SW4, the binder had dried so much during the aging that sampling a large enough piece for mounting in resin was not possible. Therefore, these samples were analyzed in powder form.

2. Selection of historical cross-sections

The C2RMF possesses an extensive collection of paint samples containing smalt, which has been collected for more than sixty years. This study deals with nine samples from paintings dating between the 16th and 18th centuries selected in this collection because they contain smalt in various alteration states. Additionally, through a collaborative effort involving C2RMF, CNRS, Delft University of Technology (TU-Delft), and the Alte Nationalgalerie (ANG) Staatliche Museen zu Berlin (SMB) - Stiftung Preussischer Kulturbesitz (SPK), six samples from two masterpieces by Caspar David Friedrich, namely "*Monk by the Sea*" and "*Abbey among Oak Trees*" were analyzed. These paintings, created between 1808 and 1810, contain smalt, marking a late use of the pigment. Interestingly, the smalt in the "Abbey among Oak Trees" appears more altered compared to its counterpart in the "Monk by the Sea". Table 2 presents a list of studied cross-sections and details about the corresponding paintings.

Figure 1: Example of studied paintings with locations of cross-sections (Table 2). A: The wedding at Cana, Paolo Veronese, 1562-1564. Louvre Museum. ©1987 RMN-Grand Palais (musée du Louvre) / Arnaudet/Schormans. B: Monk by the Sea, Caspar David Friedrich, 1808-1810. Alte Nationalgalerie. © Staatliche Museen zu Berlin, Nationalgalerie / Foto : Kristina Mösl, Francesca Schneider

All these samples were prepared as cross-sections by mounting them in polyester resin, then cutting with a saw and grinding on silicon carbide (SiC) paper. Polishing was conducted using Micromesh® polishing cloth. Historical samples were analyzed by XANES and SEM-EDX in their resin-mounted cross-section form as described above.

Table 2: Details of paint samples examined. Painting and corresponding sample locations are described in the supplementary materials.

Sample Reference	Painting Details	Sampling area
2719	Giorgio VASARI, *The Annunciation*, 1512-1574, oil on canvas, Louvre Museum	Blue area of the Virgin's mantle
6757	Paolo VERONESE, *The Wedding at Cana*, 1562-1564, oil on canvas, Louvre Museum	Clothing of the jester with parrots

12575	Pieter BRUEGEL II, *Adoration of the Kings*, 1564-1638, oil on panel, Museum of Technology of Salins-les-Bains	Faded blue garment
2177	Jan-Baptist WEENIX, *Departure of an oriental entourage,* 1621-1660, oil on canvas, Louvre Museum	Blue sky
7850	Jacob van RUISDAEL, *Wheat Field,* around 1660, oil on canvas, Lille fine arts Museum	Blue sky
6732	Salvator ROSA, *Christ risen from the dead,* 1660-1662, oil on canvas, Conde Museum	Upper right spandrel, central zone
4150	Pierre MIGNARD, *Jesus on the way to Calvary,* 1684, oil on canvas, Louvre Museum	Blue sky
P15a	Caspar David FRIEDRICH, *Abbey among Oak Trees*, 1808-1810, Oil on canvas, Alte Nationalgalerie	Ground, bottom right
P7	Caspar David FRIEDRICH, *Monk by the Sea*, 1808-1810, Oil on canvas, Alte Nationalgalerie	In a cloud on the right part of the painting

3. Selection of K-bearing compounds as reference for µ-XANES at the K K-edge

In addition to the mock-up samples and the historical cross-sections, we selected 7 K-bearing compounds to measure their K K-edge XANES spectra and use them as references. Some of these compounds: K_2SO_4, $KAl(SO_4)_2{\cdot}12H_2O$, KCl, K-oleate are common salts that could be found into paint layer [14]. Others, like KOH, KBr, KI, and KCl, are less commonly present but may form under specific environmental conditions or due to chemical reactions within the paint matrix. All salts were analyzed in powder form in the conditions described below. $KAl(SO_4)_2{\cdot}12H_2O$ spectrum is presented later in this article, the other spectra are presented in the supplementary materials.

4. Scanning electron microscopy with energy-dispersive X-ray spectroscopy (SEM-EDX)

Semi-quantitative elemental analysis and elemental mapping were performed using a JEOL 7800F scanning electron microscope equipped with two Bruker AXS 6|30 energy-dispersive X-ray detectors. Non-conductive samples were coated with platinum to avoid charge accumulation. The operational parameters included an acceleration voltage of 15 kV, a beam current of 3.6 nA, and a chamber pressure below 100 Pa. All spectra were processed using the Bruker Quantax Duo 400 analytical platform (Esprit software in its 2.5 version). Semi-quantitative analysis for elemental ratios was determined with an internal reference, and the results were expressed as oxide percentages.

5. Micro X-ray fluorescence elemental mapping (µ-XRF)

Before each µ-XANES acquisition on a given sample, elemental µ-XRF mappings were systematically conducted. The µ-XRF mappings were performed at energies of 3700 eV before µ-XANES measurements at the K K-edge and 8280 eV before µ-XANES acquisitions at the Co K-

edge. Each µ-XRF mapping covered an area of 99x99 µm², utilizing a spatial step size of 3 µm. The Dwell time for each data point during the mappings was consistently set at 0.05 seconds. This meticulous approach ensures the obtention of spatially resolved elemental information with high precision, facilitating a comprehensive understanding of the sample's composition before embarking on the subsequent XANES analyses.

6. Micro X-ray absorption near edge spectroscopy (µ-XANES) at the K and Co K-edges

The K and Co K-edge µ-XANES spectra were recorded at the European synchrotron radiation facility (ESRF) on the ID21 beamline [15, 16]. The X-ray source is a 4.8 m long low-beta straight section and is equipped with three 1.6 m long undulators: two with a 42mm period (U42) and one with a 32 mm period (U32). The U42 elements deliver maximum X-ray intensity in the energy range of 2-6 keV, while the U32 device covers the energy range of 6-9.2 keV. The energy of the beam is selected by a fixed-exit double crystal monochromator with a Si(111) ($\Delta E/E \approx 10^{-4}$) or Si(311) ($\Delta E/E \approx 10^{-5}$). For these analyses, we used one U42 undulator and the Si(111) monochromator.
The beamline could provide a focused beam with a spot size of 0.5 (ver.) x 0.7 (hor.) μm^2 at the K/Co K-edge. Spectra were acquired under vacuum in fluorescence mode within an energy range of 3580 eV to 3725 eV in 0.3 eV increments for K and from 7670 eV to 8050 eV in 0.5 eV increments for Co.
Reference data and known absorption energies allow energy calibration. The data processing and spectra evaluation, such as auto-absorption correction, background correction, and normalization, were completed using PyMca software [17].
The considerable number of spectra measured on historical samples led us to employ automated processes to separate our dataset into several analyzable groups. For this purpose, we utilized the Orange data mining software, version 3.35.0. The spectra were initially normalized. Principal Component Analysis were conducted but did not adequately separate the dataset. It was reduced and projected into a two-dimensional space using the t-SNE [18] algorithm. Subsequently, clustering was performed using a k-Means algorithm initialized with k-Means++ [19].

Results and discussion

1. SEM-SEX results

SEM-EDX analysis offered an understanding of the elemental composition of smalt grains at a microscopic level. The generated elemental maps highlight the presence and distribution of Co, K, and other relevant elements constituting the smalt grains. Figure 2 depicts examples of the maps extracted from measurements on the SL0 and SL4 mock-up samples. It illustrates a notable distinction between the unaged and aged mock-ups. In the unaged mock-up, smalt grains are evident, comprising predominantly Si, Co, K, and sodium (Na). Grains are within a binder containing Pb, consistent with the manufacturing process involving linseed oil siccatived with lead oxides.

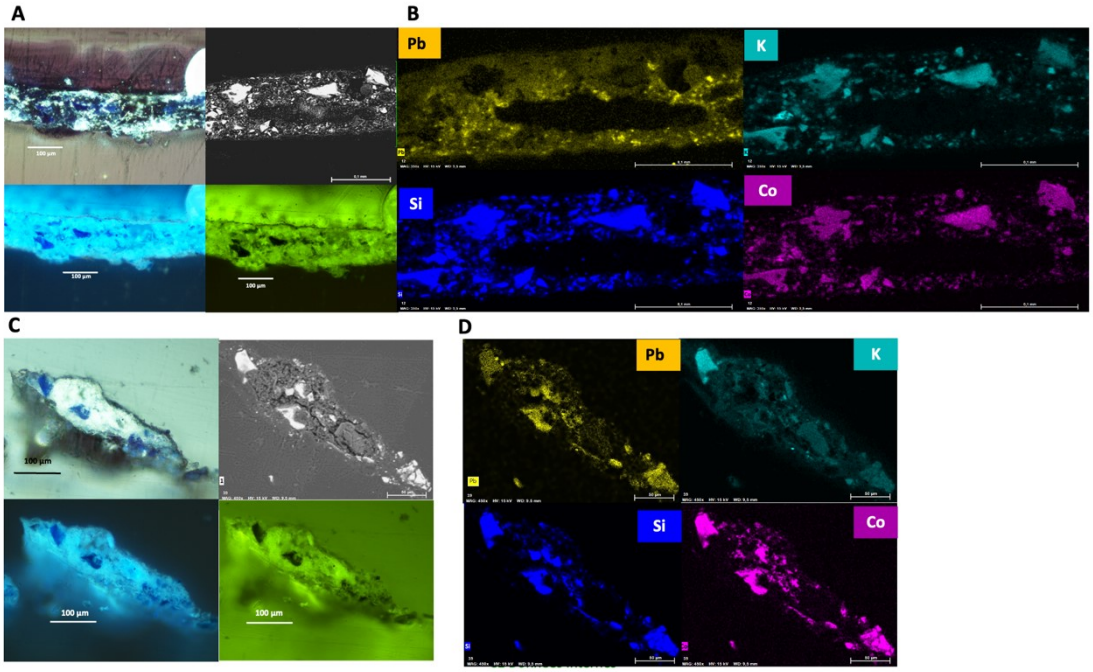

Figure 2: Observation of optical and electron microscopy of stratigraphic cross-sections of two samples prepared with siccative linseed oil, unaged (SL0) and aged for 23 days (SL4) and elemental analysis. A: Micrograph of sample SL0 under white light, near UV light and UV light and SEM image of the cross-section. B: Individual elemental maps of the cross-section of the SL0 sample. C: Micrograph of sample SL4 under white light, near UV light and UV light and SEM image of the cross-section. D: Individual elemental maps of the cross-section of the SL4 sample.

Conversely, in the aged mock-up, while the smalt grains persist, a significant redistribution of K is observed throughout the stratigraphic section. Unlike the unaged case, where K remains localized within the grains, its dispersion throughout the aged mock-up indicates a potential alteration during aging. It is also interesting to note that the Pb, in the artificially aged mock-up, is still slightly visible in the binding medium but seems more concentrated into the smalt grain. It is possible that unknown reactions occurred, leading to exchanges that allowed lead to incorporate into the glass.

This analytical technique also allowed for identifying compositional variations among smalt grains within the samples. Smalt grains were selected to determine their average composition for each analyzed mock-up (Table 3).

Table 3: Quantitative SEM-EDX analysis of the elemental composition of smalt in paint mock-ups (average over smalt grains). MC: Mean composition, SD: Standard deviation.

Sample	CoO / wt.%		SiO_2 / wt.%		K_2O / wt.%		Na_2O / wt.%		K_2O / CoO	Na_2O / CoO	K_2O / SiO_2	N a_2O / SiO_2
	MC*	SD*	MC*	SD*	MC*	SD*	MC*	SD*				
CL0	7.23	0.45	67.32	3.49	12.63	1.66	11.11	5.17	1.75	1.54	0.19	0.17
CL4	7.73	0.47	69.68	1.29	12.41	1.49	8.71	1.20	1.61	1.13	0.18	0.13
CW0	8.05	1.49	71.55	4.38	13.12	2.32	6.10	3.39	1.63	0.76	0.53	0.09
CW4	10.61	2.16	69.40	3.36	9.12	1.52	9.40	0.89	0.86	0.89	0.45	0.14
SL0	8.28	1.52	72.55	3.94	11.66	3.11	5.72	3.20	1.40	0.69	0.16	0.08
SL4	9.40	0.48	75.60	2,64	8.42	1.45	3.91	1.43	0.89	0.42	0.11	0.05
SW0	8.42	1.33	69.13	3.26	12.91	3.26	8.24	5.03	1.53	0.98	0.19	0.12
SW4	7.97	0.63	73.94	1.98	8.65	2.39	5.55	1.27	1.09	0.70	0.12	0.08

The composition of smalt grain is similar in the unaged samples, with around 75 % of Si, 7 % of CoO, 12% of K_2O. The composition in Na_2O is less homogeneous varying between 6 % and 11 %. It is also noticeable that the K_2O concentration has decreased in all the aged samples. This shows that during the aging period, K leached from the grains. The Na_2O composition also tends to decrease during the aging, suggesting that the K is not the only element that is leaching from the smalt grains. Therefore, the ratios of K_2O and Na_2O to that of CoO and SiO_2 have been calculated to estimate the weathering rate in each aged sample. This demonstrates that for these mock-up sets, the ratios decrease, indicating an alteration each time. During the artificial aging of the CL mock-up set, the Na_2O concentration decreases, and the K_2O one decrease very slightly. Mainly Na leached from the grains. The opposite is observed for the CW set, where the K_2O concentration decreases during the artificial aging but not the Na_2O one.
Overall, there is a tendency for the K_2O and Na_2O to decrease, with artificial aging showing an alteration in the aged samples. The increase in Na_2O observed in the CW set is not necessarily subdued, but it could be attributed to unknown processes occurring during the aging. Additionally, the Na composition within the smalt grains is highly inhomogeneous, as evidenced by the large standard deviations observed in the non-aged samples. This variability suggests that the Na distribution varies significantly from one grain to another, making it challenging to definitively conclude the extent of Na leaching based on the current data. Furthermore, there is heterogeneity in the levels of alteration; indeed, a relative decrease in the K to Co ratio is observed: 8 % for those with cooked linseed oil, 35.7% for mock-ups prepared with siccative linseed oil, 47.2% for those prepared with cooked walnut oil, and finally 29.5% for those with siccative walnut oil. This appears to indicate that smalt underwent more alteration when in siccative linseed oil and in cooked walnut oil compared to siccative walnut oil or cooked linseed oil. However, it would be erroneous to assert the precise state of alteration of smalt solely based on these compositions, as they do not measure the coordination state of Co^{2+} ions within the grains, and the leaching of Na^{+} ions from the grains could also influence the alteration state of the pigment.

2. µ-XANES at the Co K-edge

XANES measurements conducted at the Co K-edge precisely determined the evolution of the alteration state of the pigment in the mock-up samples. This allows the determination of the

coordination state of the cobalt ions within the grains. Figure 3 shows spectra from the set of mock-ups made with cooked walnut oil unaged and aged (CW0 and CW4).

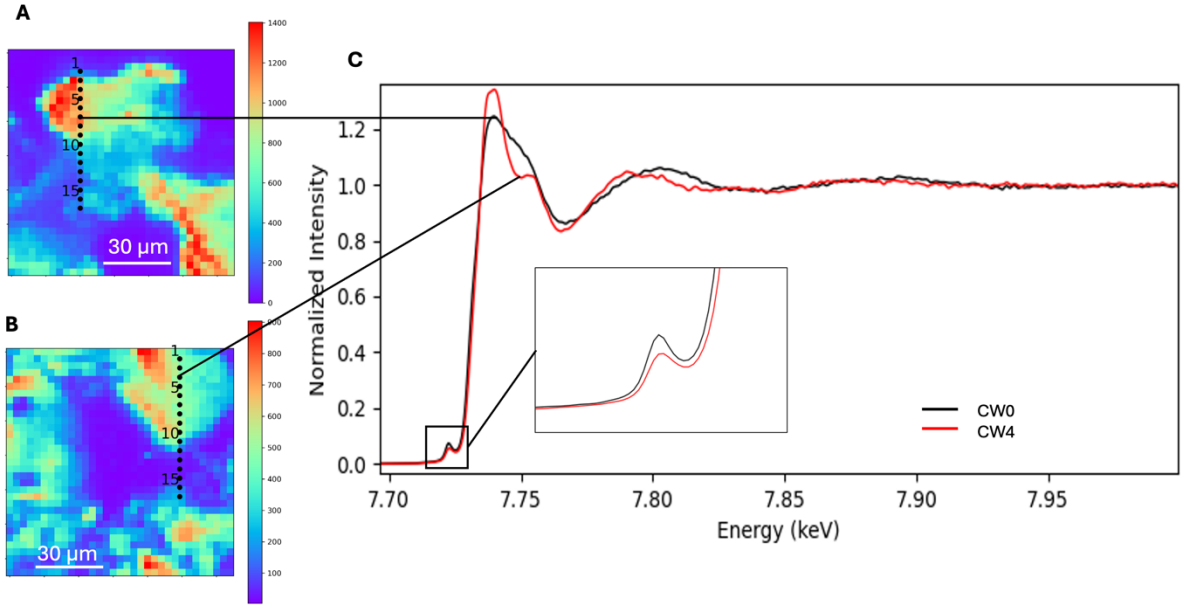

Figure 3: Comparison of µ-XANES spectra at the Co K-edge from two samples prepared with cooked walnut oil, unaged (CW0) and aged for 23 days (CW4). A: Co XRF elemental map of the CW0 sample. B: Co XRF elemental map of the CW4 sample. In A and B, the white points represent location of µ-XANES spectra. C: Comparison of µ-XANES spectra collected at the center of grains from the CW0 and CW4 samples.

The XRF elemental mapping allows the determination of the location of smalt grain in the samples thanks to elements that are constitutive of smalt, such as Co, Si, or K. Then, a µ-XANES line scan traversing a grain was performed with points spaced at intervals of 4 µm (Fig. 3A and 3B). The spectra shown in Figure 3C, derived from a grain subjected to artificial aging (CW4) and an unaged one (CW0) exhibit significant differences. It is observed that the intensity of the pre-peak centered around 7.7225 keV decreases with aging while the white line intensity increases and becomes narrower. Additionally, a shoulder around 7.755 keV appears, indicating an increase in the coordination of Co^{2+} ions from tetrahedral to octahedral coordination [7]. This demonstrates that the smalt in these samples has indeed undergone alteration during artificial aging.

It seems possible to follow the alteration state of the smalt pigment in the mock-up samples by means of µ-XANES at the Co K-edge, especially by looking at the intensities of the pre-edge peak and of the white line. These have been determined on the mean spectrum measured on each mock-up sample by measuring the intensities at 7.7225 keV (pre-edge) and at 7.7400 keV (white line) for each set. The graph in Figure 4 plots their evolutions.

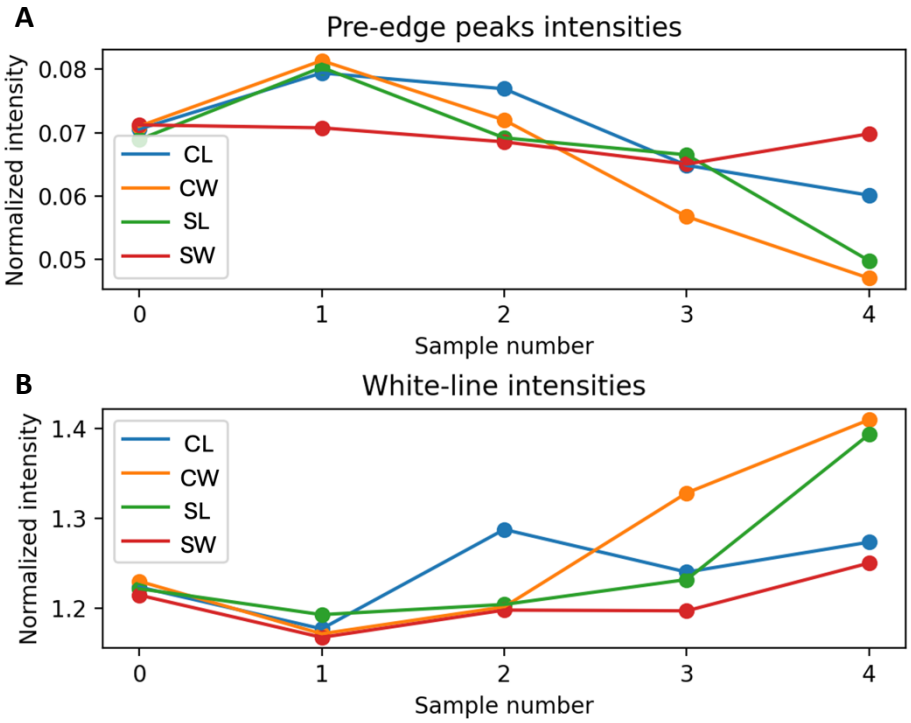

Figure 4: Evolution of the major features of Co K-edge XANES spectra from Mock-up samples. A: Evolution of the pre-edge peak intensity. B: Evolution of white line intensities

For each set of mock-ups, the intensity of the pre-edge peak tends to decrease after 23 days of aging, whereas the intensity of the white lines increase. It is interesting to note that the trends in evolution differ from one set to another. For mock-ups prepared using siccative walnut oil and those prepared using cooked linseed oil, the intensities of the pre-edge peak and the white line do not change significantly, whereas a sharp increase in the white line intensity is observed for mock-ups prepared using cooked walnut oil and those prepared using siccative linseed oil. As suggested by the study of the elemental composition of the grains using SEM-EDX, the alteration was more pronounced for samples produced with cooked walnut oil and siccative linseed oil. Samples prepared with siccative walnut oil and cooked linseed oil exhibited the lowest alteration during aging.

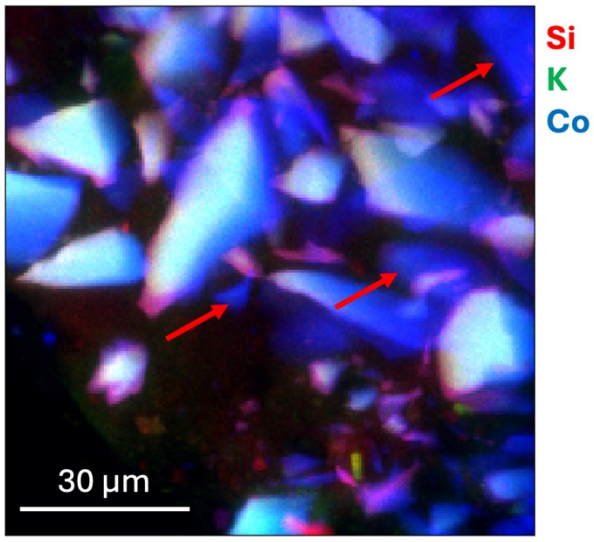

Figure 5: Si, K and Co elemental maps obtained by µ-XRF at 8.280 keV. Arrows indicate smalt grains beneath the surface visible on the Co map

If it was possible to measure the degradation state at the grain scale in mock-ups prepared as 30 µm thin sections, it becomes more complicated when the samples are thicker. Figure 5 shows the elemental maps of Si, K, and Co of historical section P7 obtained by µ-XRF at an energy of 8.280 keV. The Co mapping shows that grains of smalt can be observed beneath the surface of the section (indicated by arrows in Figure 5). This indicates that at the Co K-edge energy, X-ray penetrates beneath the surface pigments grains and probe as well grains present further inside the paint layer.

This limitation underscores the challenge in assessing individual grain coordination states in historical samples, prompting exploring alternative approaches such as K K-edge studies on mock-ups.

3. µ-XANES at the K K-edge

As for the µ-XANES at the Co K-edge, µ-XRF elemental mapping was used to determine the smalt grain location in the mock-up samples mounted as thin sections of 30 µm thickness. Then, XANES line scan was performed with points spaced at intervals of 2 µm.

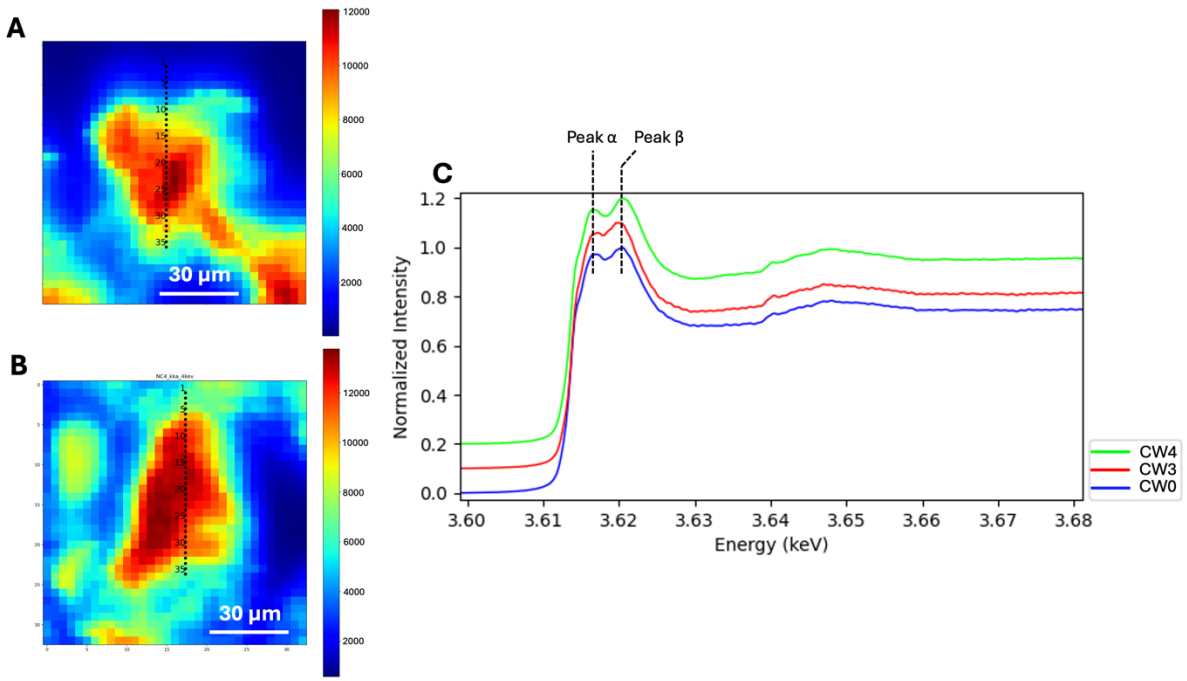

Figure 6: Comparison of µ-XANES spectra at the K K-edge from three samples prepared with cooked walnut oil, unaged (CW0), aged for 15 days (CW3) and for 23 days (CW4). A: K µ-XRF elemental map of the CW0 sample. B: K µ-XRF elemental map of the CW4 sample. In A and B, the black points represent location of µ-XANES spectra. C: K K-edge mean µ-XANES spectra of CW0, CW3, and CW4 samples.

Figures 6A, and 6B show examples of the K µ-XRF maps acquired at 3.7 keV on CW0 and CW4 samples with the location of the XANES spectra acquired. Initially, the examination of the average spectra obtained for each sample allowed their comparison. The comparison of

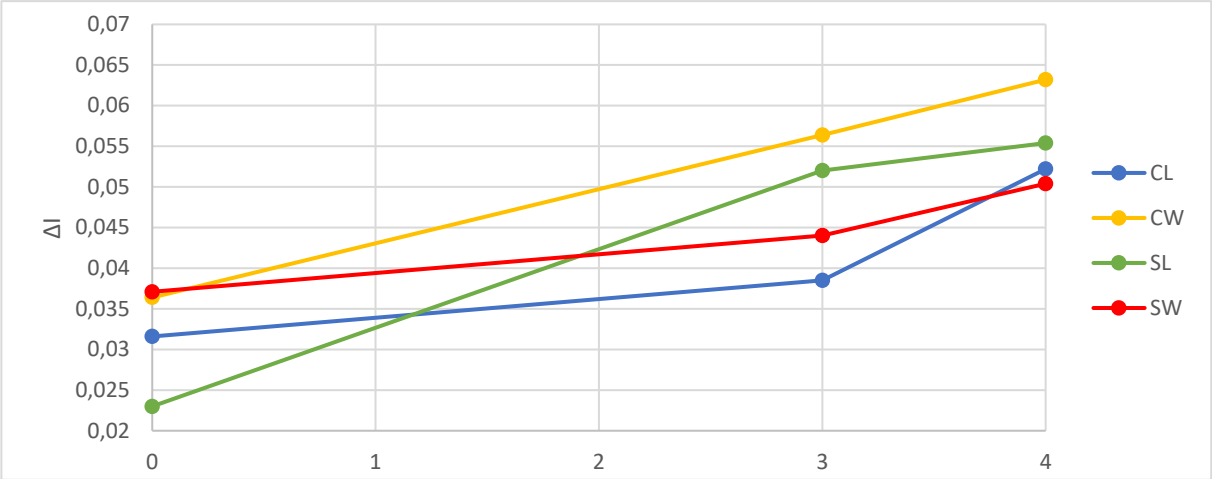

Figure 7: Evolution in intensity difference between the peaks β and α for the average K-edge µ-XANES spectra of analyzed mock-ups.

samples CW0, CW3, and CW4 is shown in Figure 6C. It can be observed that the spectra are similar, with a white line centered at 3618 eV and split into two peaks, denoted as peak α (centered around 3616 eV) and peak β (centered around 3620 eV). Upon careful observation of the three average spectra presented in the figure, some differences are noted, including i) the energy at which the inflection point occurs, which appears to shift towards higher energies with aging, ii) the widening of the white line with aging, and iii) the intensity ratio of peaks α and β, which appears to change. Indeed, the more altered the sample is, the more intense becomes peak β relative to peak α. This is verified by calculating the difference in intensity between peaks β and α for the average normalized spectra of the analyzed mock-ups from each set. Figure 7 shows the evolution of this difference as a function of the aging for each series. It is observed that for each series, the intensity difference increases with aging. Furthermore, by revisiting the results obtained at the Co K-edge threshold, it is observed that for the series where the alteration is most

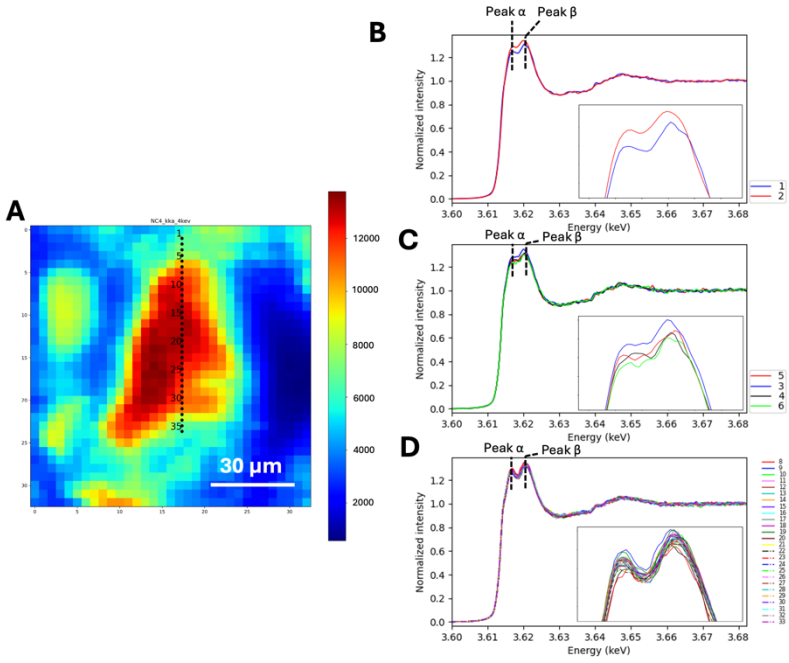

Figure 8: Comparison of XANES spectra at the K K-edge from the CW4 sample. A: K XRF elemental map with the position of the measured spectra. B: XANES spectra far from the edge of the grain. C: XANES spectra near the edge of the grain. D: XANES spectra measured inside the grain

pronounced (CW and SL), the intensity difference of XANES spectra peaks at the K K-edge also increases more significantly between measurements conducted on non-aged and aged samples. Conversely, the opposite is also verified: for series where the alteration is less pronounced (CL and SW), the intensity difference increases less.
Comparing the spectra one by one on a grain of altered smalt from sample CW4, spectral evolutions are observed, primarily differing in the shape of their white line. Figure 8B shows spectra collected far from the smalt grain (points 1-2); they exhibit a scarcely marked peak α centered around 3617 eV and a more intense peak β. Figure 8C displays spectra acquired closer to the smalt grain surface (points 3-6). They differ from those in Fig. 8B with the white line separated into three peaks: one centered around 3617 eV, another around 3618 eV, and the third around 3620 eV. Finally, spectra within the grain (points 7-33) are like those presented in Figure 6C (Fig. 8D).
This demonstrates that it is possible to monitor the alteration state of smalt using µ-XANES at the K K-edge, thus overcoming the issues related to X-ray penetration encountered at the Co K-edge. Additionally, the observation of spectra with different appearances at the edges of smalt grains can provide us with more information regarding the structural modifications undergone by K^+ ions during leaching. This could enable us to better understand the interactions between smalt and the binder.

4. Results on cross-sections of historical paintings

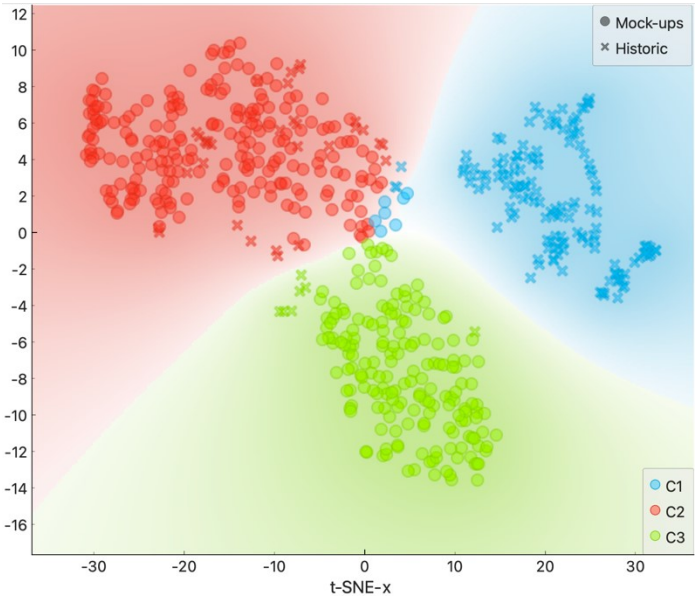

Figure 9: Results of the K-means clustering on the T-SNE projection of the dataset of 131 K K-edge XANES spectra acquired on 9 historical samples and 407 K K-edge XANES spectra acquired on mock-up samples.

Nine stratigraphic cross-sections of historical paintings were also analyzed using K and Co K-edge µ-XANES to compare the representativity of the observations made on the aged mock-ups with real samples. 131 spectra at the K-edge of K were measured on these cross-sections. Because of the complexity of historical cross-sections, the K K-edge XANES spectra are not only representative of the K^+ ions contained in smalt particles but also in other K^+-bearing phases present in the paint sample. Due to the large quantity of spectra generated, spectra measured on historical cross-section and on mock-ups were treated with a data mining approach. A first clusterization allowed the identification of three distinct clusters, as shown in Figure 9.
Cluster 1 predominantly contains spectra from historic cross-section, while cluster 2 predominantly contains spectra from mock-up samples. Cluster 3 contains a mixture of spectra from both historic cross-sections and mock-ups.
Observation of the average spectra of each cluster (Figure 10) reveals a difference between the spectra of clusters 2 and 3, resembling the spectra observed on smalt grains (Figure 6 and

8), whereas those of cluster 1 are distinct. In this figure, the average spectrum of each of these clusters is represented, with the maximum deviations from the average spectrum indicated.

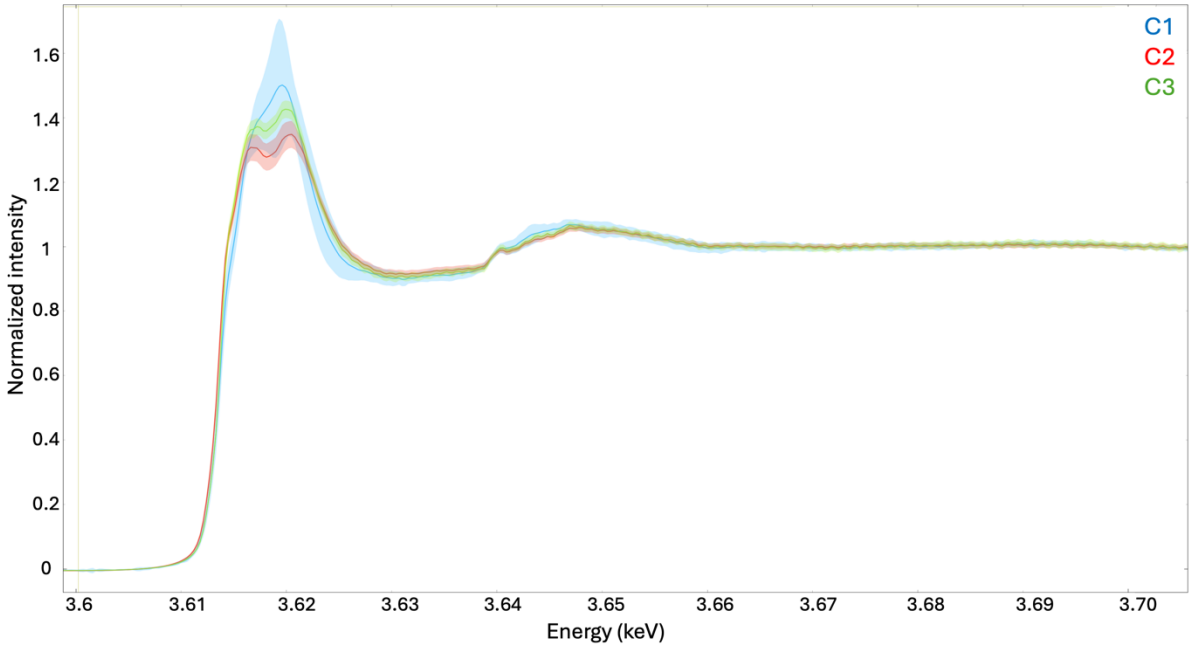

Figure 10: Mean K K-edge spectra of clusters 1,2 and 3

4.1 Analysis of cluster 2 and 3 corresponding to smalt in mock-ups and historical cross-sections

Cluster 2 contains 213 spectra. Among them, 181 are basically from the mock-up samples CL0, CL3, SL0, CW0, SW0 and SW3, which are the mock-ups where smalt is well-preserved. This cluster also contains 32 spectra from historical cross-sections (P7, 4150, 6732, 12575) all

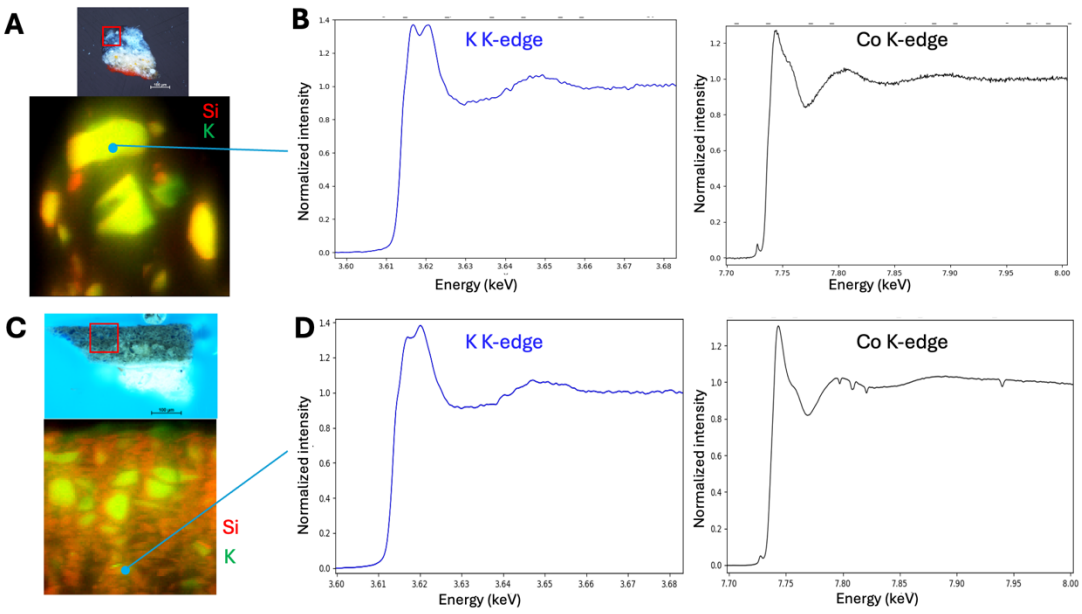

Figure 11: Analyses of µ-XANES from clusters 2 and 3. A: Micrograph of the P7 cross-section and µ-XRF elemental map of Si and K within the red-framed area. B: µ-XANES spectra at the K K-edge (left) and the Co K-edge (right) of the analyzed point shown in Figure 11A. C: Micrograph of the 2719 cross-section and µ-XRF elemental map of Si and K within the red-framed area. D: µ-XANES spectra at the K-edge (left) and the Co K-edge (right) of the analyzed point shown in Figure 11C.

exhibiting a pretty intense peak α and a relatively low-intensity difference between peaks β and α. In these historical cross-sections, these spectra were registered in areas where the smalt is still well-preserved, as exemplified in Figures 11A and B. The µ-XANES spectrum of the Figure 11B at the K K-edge was measured in a grain containing a significant amount of K, originating from a paint layer still appearing blue (sample P7). Additionally, figure 14B also illustrates the average spectrum of analyses conducted at the Co K-edge on the same smalt grain, displaying a characteristic spectrum of minimally altered smalt.
Clusters 3, on the other hand, contain a total of 219 spectra and exhibit a less intense peak α compared to the spectra in cluster 2, resulting in a more significant intensity difference between peaks β and α. 209 of these spectra were measured in mock-ups samples were smalt is weathered (CL3, CL4, SL3, SL4, CW3, CW4 and SW4). The ten last spectra were measured in three different historic cross-sections, among which sample 2719 shown in Figure 11 C and D. The average Co K-edge µ-XANES spectrum from this cross-section show an intermediate alteration state (Figure 11D). XANES at the K K-edge measured on grains exhibit a similar appearance to that shown in the example of Figure 11D: a less developed peak α and a more significant intensity difference between peak β and α, thus belonging to clusters 3 which are indicative of an intermediate state of weathering.

4.2 Analysis of cluster 1 corresponding to different K-bearing compounds in historical cross-section including smalt

The cluster 1 predominantly contains spectra from historical samples, which exhibit a wide variation around the cluster's mean spectrum (Figure 10). The historical cross-sections, being complex systems, contain other compounds compared to the laboratory-made mock-ups. Thus, XANES spectra at the K K-edge exhibiting different patterns from those presented so far have also been measured in these cross-sections. It was isolated from the other two, and a new clustering approach was applied to it in order to gain a deeper understanding of this cluster. This clustering yielded six distinct groups (Figure 12).

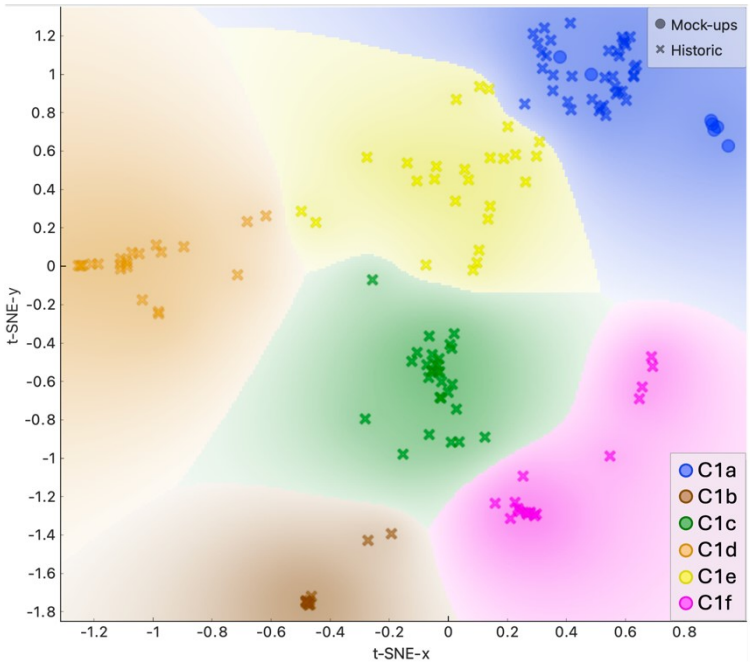

Figure 12: Results of the K-means clustering on the T-SNE projection of the dataset of 137 K K-edge XANES spectra of cluster 1.

Cluster 1a, 1c, 1e contains K K-edge µ-XANES spectra characteristic of smalt grains and characterized by an almost non-existent peak α and a large intensity difference between peak β and α. These clusters comprise 76 spectra from cross-sections P7, P15a, 2177, 2719, 4150, 6732 and 6757, 7850. These spectra were measured on smalt grains where almost all of the K contained has been leached, as depicted in Figure 13B. These grains are thus in a highly altered state, as evidenced by the average XANES spectrum at the Co K-edge presented in

Figure 13C for the example provided (sample 6757). It is possible that the degree of degradation of the smalt grains on which these spectra were measured is more advanced than the highest state of alteration of the smalt in the mock-ups. It would explain why the initial clustering did not classify them with the mock-ups.

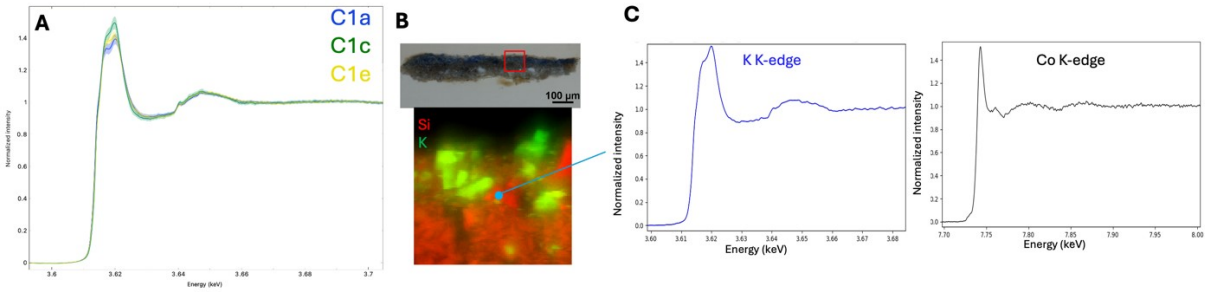

Figure 13: Analyses of µ-XANES from clusters 1a, 1c and 1e. A: Mean K K-edge µ-XANES spectra of the clusters. B: Micrograph of the 6757 cross-section and µ-XRF elemental map of Si and K within the red-framed area. C: µ-XANES spectra at the K K-edge (left) and the Co K-edge (right) of the analyzed point shown in Figure

Cluster 1b contains spectra exhibiting a white line with two peaks: a slightly intense peak centered around 3.616 keV and a very intense peak centered around 3.619 keV. Three characteristic oscillations were observed after the white line, centered around 3.628, 3.645, and 3.644 keV (Figure 14A). These spectra do not resemble any other measured spectrum or reference analyzed during the experiment. However, they were only found in two cross-sections, notably in P7 (Figure 14B). The spectra from cluster 1b were measured in areas containing dispersed K but no Si, indicating they are outside the smalt grains. Moreover, they were found only close to the uppermost parts of the paint stratigraphy and, therefore, the surface of the paintings. These spectra may represent a product of the transformation of K^+ ions that have left the smalt grains and migrated to the surface of the painting.

Cluster 1d also contains spectra where the white line has a single peak, this time centered around 3.617 keV, with a slight shoulder around 3.630 keV (Figure 14C). These spectra were measured on two cross-sections, 2177 and P15a. Cross-section P15a is depicted in Figure 14D, showing the locations where the spectra of this cluster were measured. A significant similarity was observed in comparing the obtained spectra to a reference of $KAl(SO_4)_2 \cdot 12H_2O$ (Figure 14E). These two cross-sections contain K alum, which could have been added as such by the

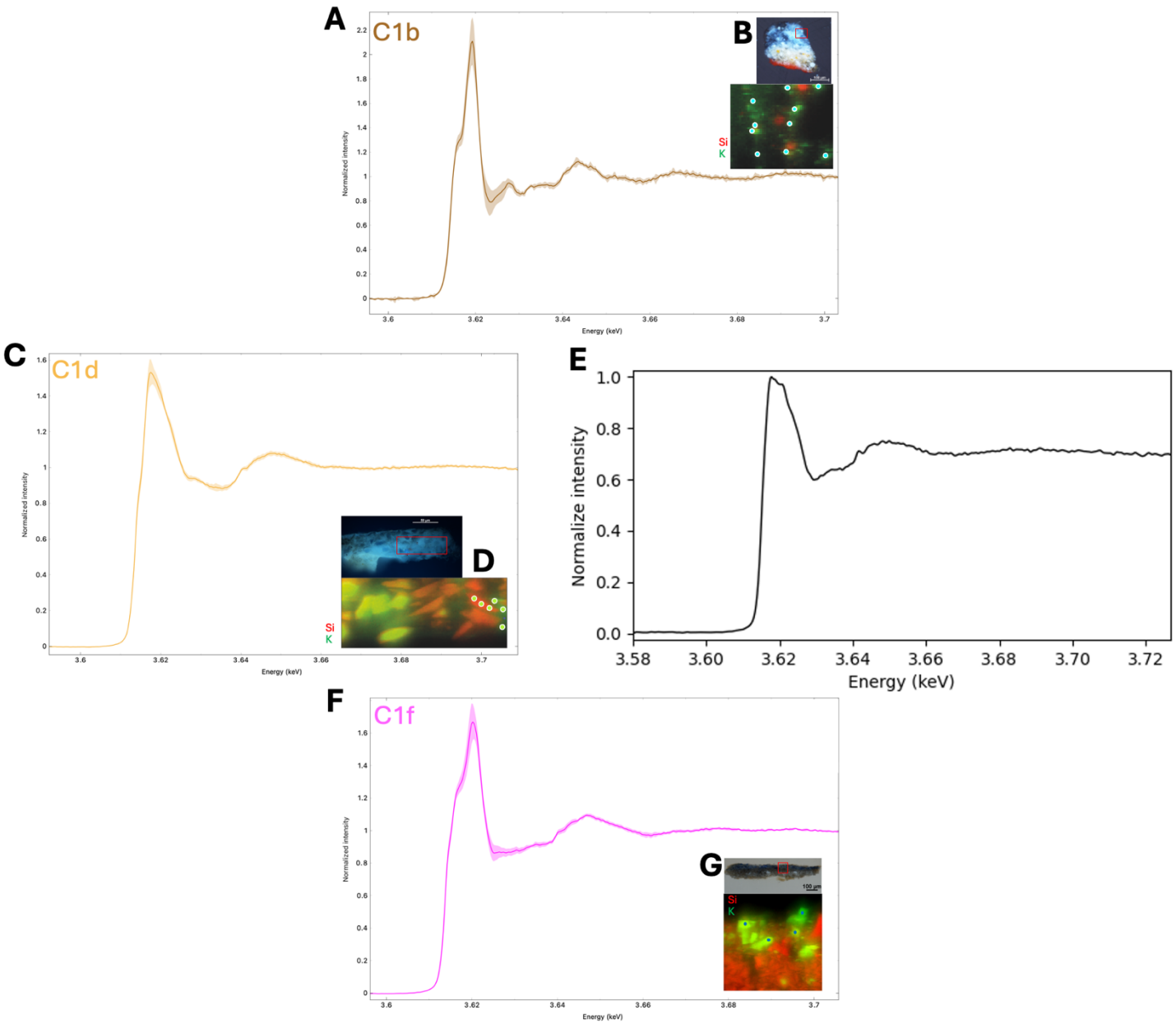

Figure 14: Analyses of K K-edge XANES clusters 1b,1d and 1f. A: Mean spectrum of spectra from cluster 1b. B: Micrograph of the P7 cross-section and µ-XRF elemental map of Si and K within the red-framed area; locations of the spectra measured on the sample and belonging to cluster 1b are indicated by dots. C: Mean spectrum of spectra from cluster 1d. D: Micrograph of the P7 cross-section and µ-XRF elemental map of Si and K within the red-framed area; locations of the spectra measured on the sample and belonging to cluster 1d are indicated by dots. E: K K-edge µ-XANES spectrum of a $KAl(SO_4)_2{\cdot}12H_2O$ reference. F: Mean spectrum of spectra from cluster 1f. G: Micrograph of the 6757 cross-section and µ-XRF elemental map of Si and K within the red-framed area, locations of the spectra measured on the sample and belonging to cluster 1f are indicated by dots.

painter or could have formed *in-situ* because of leaching K from smalt grains.

Finally, cluster 1f contains spectra exhibiting a white line with a single peak centered around 3.620 keV and a broad width. They also display a shoulder at approximately 3.616 keV (Figure 14F). These spectra were measured on only two cross-sections: 2719 and 6757, originating respectively from "The Annunciation" by Giorgio Vasari and "The Wedding at Cana" by Paolo Veronese. The locations of the spectra of this cluster measured on cross-section 6757 were shown in Figure 14G. They were found in areas containing an important level of K and less Si than in smalt grains. SEM-EDX analyses, as well as µ-XRF analysis (supplementary material),

reveal the presence of lapis lazuli in these two cross-sections. It is, therefore, highly probable that these spectra are corresponding to the K K-edge features of lapis lazuli.

Conclusion

This study highlights the complex alteration processes affecting smalt pigment in historical artworks. Through µ-XANES analyses at the K and Co K-edges, coupled with SEM-EDX and µ-XRF techniques, distinct spectral signatures associated with different stages of smalt degradation and related chemical transformations were identified. Our results reveal the nuanced structural changes occurring within smalt grains as they undergo alteration, providing valuable insights into the degradation mechanisms and the factors influencing pigment stability in paint layer. It is still important to note that the environmental conditions applied during artificial aging differ from those in natural aging, and therefore, specific conclusions regarding long-term pigment stability in historical contexts should be approached with caution.

Our analysis of mock-up samples has revealed new insights into the differential alteration rates of smalt pigment under various oily based binding media. Specifically, it was found that smalt degraded more rapidly in samples employing cooked walnut oil and lead oxide siccative linseed oil compared to those utilizing cooked linseed oil and walnut oil siccative with lead oxide. This observation underlines that the binding medium composition noteworthy influences the smalt degradation kinetics within paint layers.

Furthermore, the comparison between historical cross-sections and laboratory mock-ups has demonstrated the efficiency of XANES at the K K-edge in tracking the alteration state of smalt at a grain-scale level. This approach not only elucidates the impact of alteration on the local environment of Co^{2+} ions but also highlights the influence of K^{+} migration on pigment degradation.

Moreover, the identification of K alum and other transformation products in specific cross-sections underscores the dynamic nature of pigment alteration processes within historical artworks. The spatial distribution of these transformation products, particularly near the surface of paintings, suggests a potential migration pathway for leached K^{+} ions and highlights the importance of understanding surface interactions in the context of artwork conservation and restoration.

Identifying additional products observed in historical samples using K K-edge XANES and conducting more in-depth studies on the composition of binders and their changes in mock-ups are further research questions. Such further investigation aims at better understanding the observed differences in smalt alteration in different paintings that seem independent of the age of the painting.

Thus, the results obtained through XANES analyses at the K K-edge on historical samples align with those obtained on our model samples. The structural changes in the silicate matrix of the smalt grains occurring during their alteration not only influence the immediate environment of Co^{2+} ions but also affect K^{+} ions that have not yet leached out.

This research is not only interesting for studying the alteration of smalt but also in general all K-bearing glasses and opens therefore interesting new research avenues.

Bibliography

1. Delamare F (2009) Aux origines des bleus de cobalt : les débuts de la fabrication du saffre et du smalt en Europe occidentale. crai 153:297–315. https://doi.org/10.3406/crai.2009.92472
2. Stege H (2004) Out of the blue ? Zeitschrift für Kunsttechnologie: ZKK 18:121–142
3. Mühlethaler B, Thissen J (1969) SMALT. Studies in Conservation 14:47–61. https://doi.org/10.1179/sic.1969.005
4. Spring M, Higgitt C, Saunders D (2005) Investigation of Pigment-Medium Interaction Processes in Oil Paint containing Degraded Smalt. National Gallery Technical Bulletin 26:
5. Hartwig J (2001) De la fabrication et de l'utilisation du Safre ou Zaffera (cobalt) et du Smalte , par les verriers durant les XVI ème,XVII ème et XVIII ème siècles. Verre 7:
6. Robinet L, Spring M, Pagès-Camagna S (2013) Vibrational spectroscopy correlated with elemental analysis for the investigation of smalt pigment and its alteration in paintings. Anal Methods 5:4628. https://doi.org/10.1039/c3ay40906f
7. Robinet L, Spring M, Pagès-Camagna S, et al (2011) Investigation of the Discoloration of Smalt Pigment in Historic Paintings by Micro-X-ray Absorption Spectroscopy at the Co K-Edge. Analytical Chemistry 83:5145–5152. https://doi.org/10.1021/ac200184f
8. Reiche I, de Mecquenem C, Eveno M (2022) L'utilisation du smalt et son altération dans les peintures des collections françaises. In: Les bleus et les verts : couleurs et lumières, Hermann. pp 75–88
9. de Mecquenem C, Eveno M, Alfeld M, et al (2023) A multimodal study of smalt preservation and degradation on the painting "Woman doing a Libation or Artemisia" from an anonymous painter of the Fontainebleau School. The European Physical Journal Plus 138:185. https://doi.org/10.1140/epjp/s13360-023-03799-4
10. Ganio M, Daly N, Patterson C, et al (2019) Tracking smalt degradation: the role of potassium and cobalt structural changes and distribution in the glass matrix on discoloration
11. Laurence de Viguerie, Guylaine Ducouret, François Lequeux, et al (2009) Historical evolution of oil painting media: A rheological study. Comptes Rendus Physique 10:612–621. https://doi.org/10.1016/j.crhy.2009.08.006
12. Lazzari M, Chiantore O (1999) Drying and oxidative degradation of linseed oil. Polymer Degradation and Stability 65:303–313. https://doi.org/10.1016/S0141-3910(99)00020-8
13. Cianchetta I, Colantoni I, Talarico F, et al (2012) Discoloration of the smalt pigment: experimental studies and ab initio calculations. J Anal At Spectrom 27:1941. https://doi.org/10.1039/c2ja30132f
14. Arnold A, Zehnder K (1991) Monitoring wall paintings affected by soluble salts. Getty Conservation Institute Marina Del Rey
15. Cotte M, Pouyet E, Salomé M, et al (2017) The ID21 X-ray and infrared microscopy beamline at the ESRF: status and recent applications to artistic materials. J Anal At Spectrom 32:477–493. https://doi.org/10.1039/C6JA00356G
16. Salomé M, Cotte M, Baker R, et al (2013) The ID21 Scanning X-ray Microscope at ESRF. J Phys: Conf Ser 425:182004. https://doi.org/10.1088/1742-6596/425/18/182004
17. Solé VA, Papillon E, Cotte M, et al (2007) A multiplatform code for the analysis of energy-dispersive X-ray fluorescence spectra. Spectrochimica Acta Part B: Atomic Spectroscopy 62:63–68. https://doi.org/10.1016/j.sab.2006.12.002
18. van der Maaten L, Hinton G (2008) Viualizing data using t-SNE. Journal of Machine

Learning Research 9:2579–2605
19. Arthur D, Vassilvitskii S (2007) K-Means++: The Advantages of Careful Seeding

Acknowledgements

We would like to thank the University of Versailles Saint-Quentin-en-Yvelines and University School of Humanities, Creation, Heritage, Investment of Future ANR-17- EURE-0021 - Fondation des Sciences du Patrimoine and the UVSQ University for their support through the MARCS project. A special thank goes to Emmanuel Poireault, who has been playing a crucial role in the *Fondation des Sciences du Patrimoine,* for his unwavering interest and assistance throughout the project. We would also like to thank ESRF synchrotron facility for providing the facilities with synchrotron radiation on beam line ID21 (experiment HG211).

Statement and Declarations

Author contributions

Clément de Mecquenem (CdM), Myriam Eveno (ME) and Ina Reiche (IR) conceived and designed the programme. Material preparation, data collection and analysis were performed by CdM, ME, Damaris Zurbach, Kristina Mösl, Marine Cotte and IR. The first draft of the manuscript was written by CdM, ME and IR. All authors commented on previous versions of the manuscript. All authors read and approved the final manuscript.

Competing Interests

This work benefited from support from the Krupp foundation and the French State managed by the National Research Agency under the “Investment for the Future” program integrated into France 2030, under reference ANR-17_EURE_0021, University Research School Paris Seine Humanity, Creation, Heritage – Fondation des sciences du Patrimoine.

The authors have no relevant non-financial interest to disclose.

Data Statements

The datasets generated during and/or analysed during the current study are available from the corresponding author on reasonable request. A part of the processed data is also available on the supplementary materials